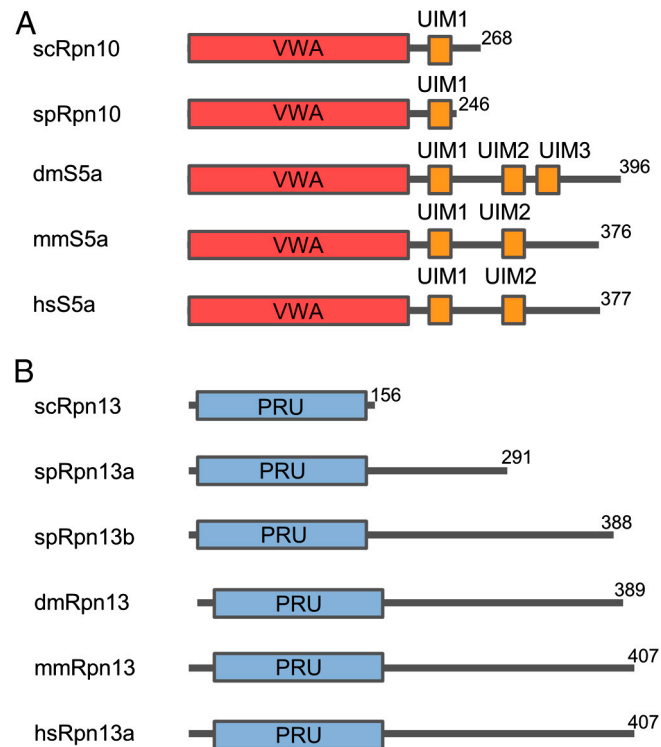# Supporting Information

Sakata et al. 10.1073/pnas.1119394109

Fig. S1. Domain structures of Rpn10 and Rpn13 from various species. (*A*) Rpn10 consists of the N-terminal von Willebrand factor A domain (red) and C-terminal UIM domain (orange). *Saccharomyces cerevisiae* Rpn10 contains only one ubiquitin-interacting motif (UIM), whereas human and Drosophila S5a contain two and three UIMs, respectively. (*B*) The N-terminal pleckstrin-like receptor of ubiquitin domain of Rpn13 is generally conserved among species, whereas the C-terminal region which interacts with UCH37 is absent in *S. cerevisiae* and *Schizosaccharomyces pombe*.

Wild type

rpn10Δ

rpn13Δ

rpn10Δrpn13Δ

100 nm

100 nm

100 nm

100 nm

Fig. S2. Electron micrographs of *S. cerevisiae* 26S proteasome purified from wild-type and deletion mutants cells. Raw images of wild-type and mutated 26S proteasome. Examples of molecular images selected for analysis are circled (*Upper Left*, wild type).
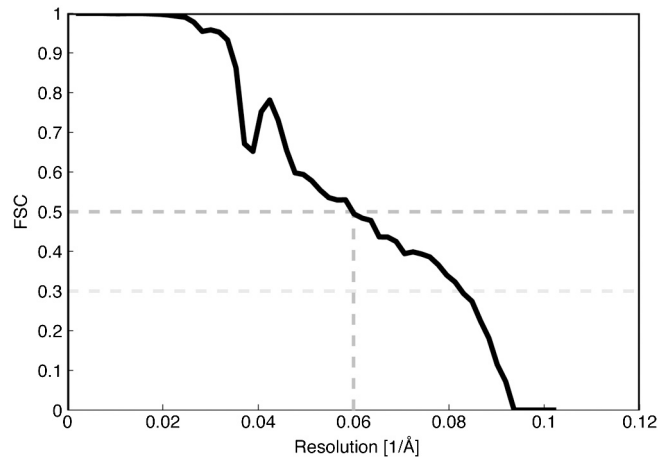
Fig. S3. Fourier shell correlation (FSC) curve of the wild-type 26S proteasome. The resolution of the final reconstruction was estimated to be 16.8 Å using the FSC 0.5 cutoff criterion or 12.1 Å for FSC = 0.3.
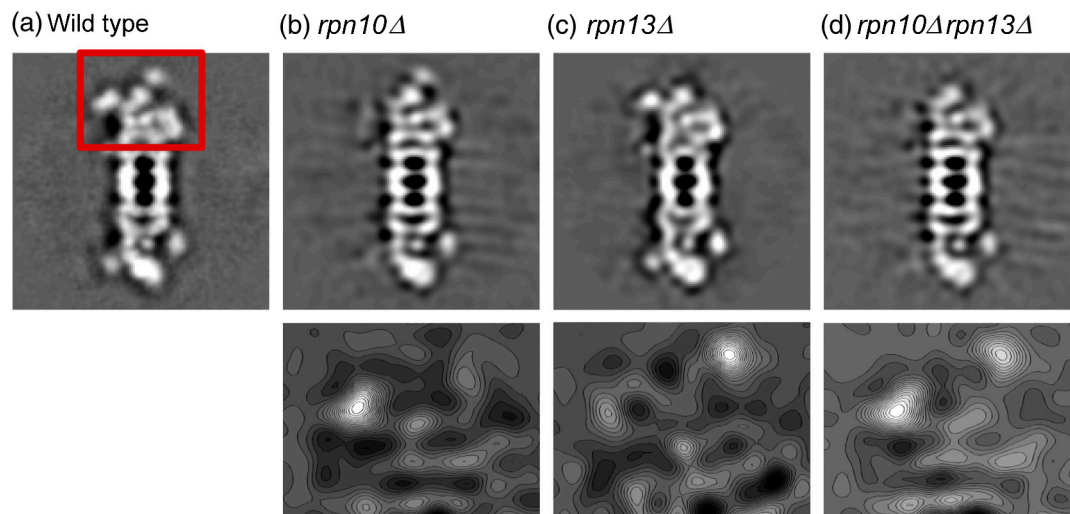
Fig. S4. Structural comparisons between wild-type and deletion mutants. A projection of total averaged structures (upper row) and difference maps (lower row) are represented in the same orientation. 19S regulatory particles (RPs) are marked with a rectangle.

Fig. S5. (*A*) Structural comparisons of 26S proteasome from *S. cerevisiae* (a), *Drosophila melanogaster* (b) (1), and *Schizosaccharomyces pombe* (c) (2). Only *S. cerevisiae* 26S proteasome possesses an additional bulbous protrusion at the apex of the RP. (*B*) Three-dimensional classification of 26S proteasome focused on Rpn13 localization. Particles are classified into four classes by the difference of the focused region, which is shown by mesh. Approximately 50% of all particles from *D. melanogaster* and *S. pombe* exhibited an extra density at the Rpn13 site, whereas all particles possess the extra density in *S. cerevisiae*. Rpn13 is not observed in maps from the complete set of *S. pombe* and *D. melanogaster* particles because of the low abundance and flexibility of Rpn13 in these species.

1 Nickell S, et al. (2009) Insights into the molecular architecture of the 26S proteasome. *Proc Natl Acad Sci USA* 106:11943–11947.
2 Bohn S, et al. (2010) Structure of the 26S proteasome from Schizosaccharomyces pombe at subnanometer resolution. *Proc Natl Acad Sci USA* 107:20992–20997.

Fig. S6. Three-dimensional classification of 26S proteasome focused on the C terminus of Rpn10, applied to *S. cerevisiae* (a) and *D. melanogaster* (b) proteasome and *D. melanogaster* proteasome labeled by Dsk2 (c). Particles are classified into six classes based on the difference in the focused region, which is shown by mesh. Additional density is observed in one class of (c) (red circle). The C terminus of UIM is located above the coiled coil of Rpt4/Rpt5.

Table S1. Yeast strains used in this study

Strain	Genotype	Reference
W303-1A	MATa ura3-1, trp1-1, leu2-3,112, his3-11,15, ade2-1, can1-100	our stock
YYS40	MATa RPN11-3FLAG::HIS3	from 1
YYS1027	MATa Δrpn10::HphMX rpn11::RPN11-3FLAG-HIS3	this study
YYS1029	MATα Δrpn13::KanMX rpn11::RPN11-3FLAG-HIS3	this study
YYS1030	MATa Δrpn10::HphMX Δrpn13::KanMX4 rpn11::RPN11-3FLAG-HIS3	this study

All strains had the W303 strain as background.

1 Saeki Y, Isono E, Toh EA (2005) Preparation of ubiquitinated substrates by the PY motif-insertion method for monitoring 26S proteasome activity. *Methods Enzymol* 399:215–227.